Developmental Cell
Article

Synergistic Function of E2F7 and E2F8 Is Essential for Cell Survival and Embryonic Development

Jing Li,[1,2] Cong Ran,[1,2] Edward Li,[1,2] Faye Gordon,[1,2] Grant Comstock,[1,2] Hasan Siddiqui,[1,2] Whitney Cleghorn,[1,2] Hui-Zi Chen,[1,2] Karl Kornacker,[3] Chang-Gong Liu,[1] Shusil K. Pandit,[4] Mehrbod Khanizadeh,[4] Michael Weinstein,[1,2] Gustavo Leone,[1,2,*] and Alain de Bruin[1,2,5]

[1]Human Cancer Genetics Program, Department of Molecular Virology, Immunology and Medical Genetics, Comprehensive Cancer Center, College of Medicine and Public Health

[2]Department of Molecular Genetics, College of Biological Sciences

[3]Division of Sensory Biophysics

The Ohio State University, Columbus, OH 43210, USA

[4]Department of Pathobiology, Faculty of Veterinary Medicine, Utrecht University, 3584 CL Utrecht, The Netherlands

[5]Present address: Department of Pathobiology, Faculty of Veterinary Medicine, Utrecht University, 3584 CL Utrecht, The Netherlands.

*Correspondence: gustavo.leone@osumc.edu

DOI 10.1016/j.devcel.2007.10.017

SUMMARY

The *E2f7* and *E2f8* family members are thought to function as transcriptional repressors important for the control of cell proliferation. Here, we have analyzed the consequences of inactivating *E2f7* and *E2f8* in mice and show that their individual loss had no significant effect on development. Their combined ablation, however, resulted in massive apoptosis and dilation of blood vessels, culminating in lethality by embryonic day E11.5. A deficiency in *E2f7* and *E2f8* led to an increase in *E2f1* and p53, as well as in many stress-related genes. Homo- and heterodimers of E2F7 and E2F8 were found on target promoters, including *E2f1*. Importantly, loss of either *E2f1* or *p53* suppressed the massive apoptosis in double-mutant embryos. These results identify E2F7 and E2F8 as a unique repressive arm of the E2F transcriptional network that is critical for embryonic development and control of the E2F1-p53 apoptotic axis.

INTRODUCTION

A large body of work suggests that E2Fs function to activate and repress the transcription of many essential genes involved in cell proliferation, apoptosis, and differentiation (Dimova and Dyson, 2005). The effects of deregulated E2F activity are pleiotropic and vary in different experimental settings. A decrease in E2F activity is generally associated with a reduction in the proliferation capacity of cells (Leone et al., 1998; Humbert et al., 2000b; Wu et al., 2001), whereas an increase in E2F activity is often associated with inappropriate cell proliferation and/or apoptosis (DeGregori et al., 1997). The regulation of E2F activity during the cell cycle is thought to be critical for cellular homeostasis. Thus, a significant amount of genetic currency has been invested to finely control E2F activity in cells, including by direct binding of the Rb tumor suppressor, by transcription, by posttranscriptional mechanisms involving miRNAs, and by posttranslational mechanisms involving protein degradation, phosphorylation, and acetylation (Muller and Helin, 2000; O'Donnell et al., 2005).

Further complexity in the regulation of E2F function has been afforded by the evolution of numerous family members and isoforms. The mammalian E2F proteins are encoded by eight distinct genes (E2F1-8), and specific roles for each family member in controlling cell cycle transitions and apoptosis have been reported (Bracken et al., 2004; DeGregori and Johnson, 2006). Based on structure-function studies and sequence analysis, the E2F family can be conveniently divided into two general subclasses, transcription repressors and activators. Members of the activator subclass, consisting of E2F1, E2F2, and E2F3a, accumulate late in G_1 and are transiently recruited to E2F-binding elements on target promoters and participate in their acute activation. Consistent with an important function for activator E2Fs in regulating gene expression during G_1-S, their overexpression in quiescent cells can potently transactivate many E2F-responsive genes and drive cells to enter S phase (DeGregori et al., 1997). Conversely, the combined loss of the three activators results in a decrease of E2F-target gene expression and a severe block in cell proliferation (Wu et al., 2001). The repressor subclass consists of E2F3b, E2F4, E2F5, E2F6, E2F7, and E2F8. A subset of this group that includes E2F3b, E2F4, and E2F5 serves to recruit Rb-related pocket proteins and associated corepressors to target promoters during G0 and to repress their expression (Attwooll et al., 2004). As cells are stimulated to enter the cell cycle, cyclin-dependent kinases (CDKs) phosphorylate pocket proteins, resulting in dissociation of E2F-pocket protein repressor complexes and derepression of E2F-target genes (Muller and Helin, 2000; Seville et al., 2005). The E2F6 repressor is part of a multisubunit complex that includes polycomb group proteins as well as Mga and Max, and appears to act on a different subset of target genes than E2F4 (Ogawa et al., 2002; Giangrande et al., 2004). The mechanism of how E2F7 and E2F8 repress gene expression is less clear. While the molecular basis for how E2F repressors and activators orchestrate the acute induction of E2F targets as cells transit through G_0-G_1-S is fairly well understood, how E2F-target genes are subsequently downregulated as cells proceed through S-G_2 phases of the cell cycle is not known.

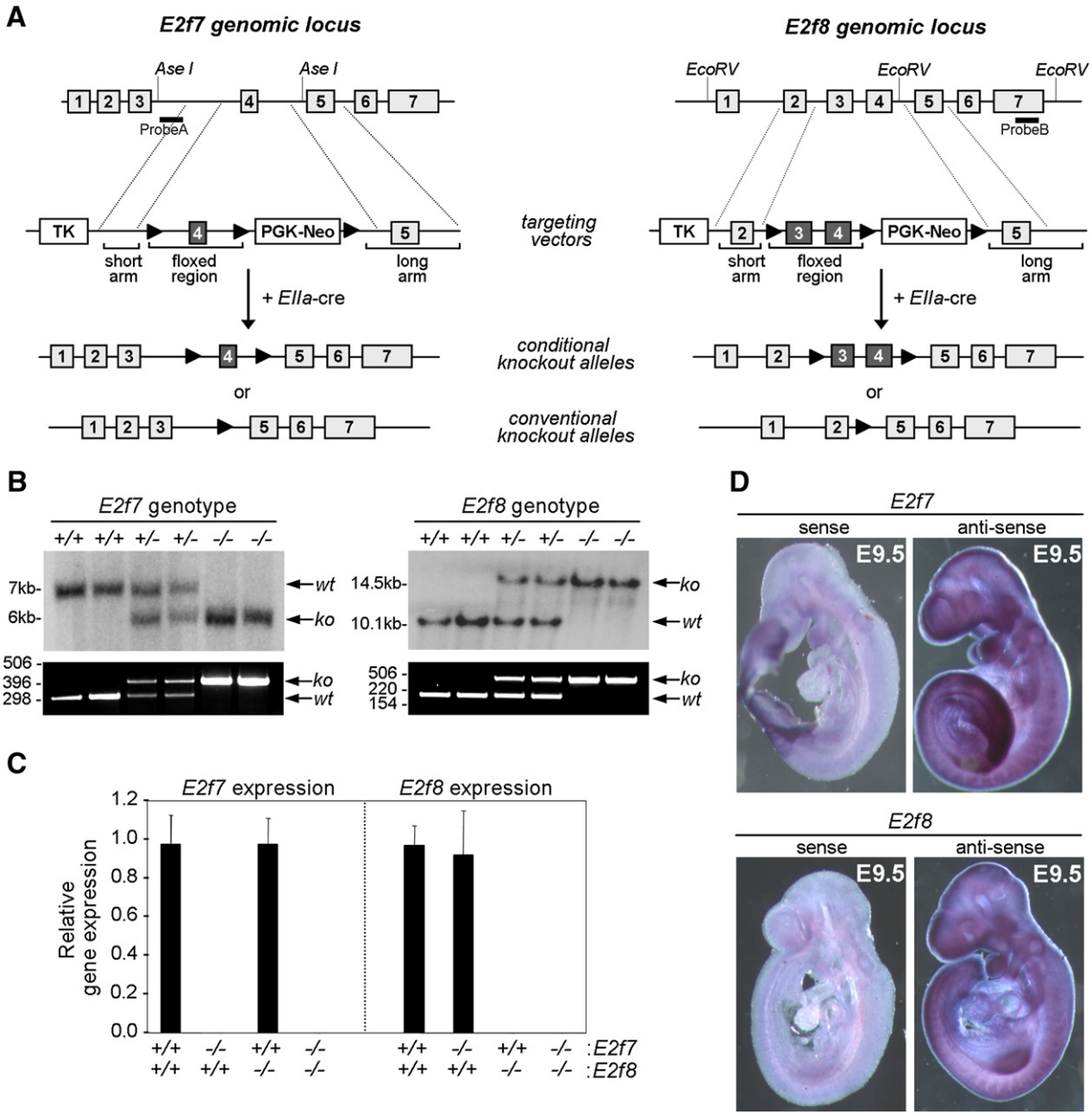

Figure 1. Generation of *E2f7* and *E2f8* Knockout Mice

(A) Targeting strategies used to inactivate *E2f7* (left) and *E2f8* (right). Top panels: partial exon/intron structures of the *E2f7* and *E2f8* genes. The black bars indicate the position of probes used for Southern analysis. Middle panels (targeting vectors): position of the *TK* and *Neo* cassettes, as well as *loxP* sites (filled triangles) are indicated. Bottom two panels (conditional knockout alleles and conventional knockout alleles): illustrate the two desired alleles resulting from possible recombination events.

(B) Top panels: Southern analysis of genomic DNA isolated from conventional knockout mice using *AseI* for *E2f7* (left) and *EcoRV* for *E2f8* (right), and hybridized using probes A and B, respectively. Bottom panels: genotyping of tail DNA was performed using allele-specific PCR primers.

(C) Real-time RT-PCR analysis of *E2f7* or *E2f8* expression in embryos with the indicated genotypes using primers described in Figure S7. Wild-type samples were normalized to 1. Data are presented as the average ± SD-fold reduction in samples analyzed in triplicate.

(D) Wild-type E9.5 embryos were subjected to whole-mount in situ hybridization using sense and antisense probes specific to *E2f7* (top panels) and *E2f8* (bottom panels).

The E2F7 and E2F8 proteins are conserved in mice and humans, and related E2F-like proteins exist in *Arabidopsis* (Kosugi and Ohashi, 2002; Mariconti et al., 2002; de Bruin et al., 2003; Di Stefano et al., 2003; Logan et al., 2004, 2005; Christensen et al., 2005; Maiti et al., 2005). These two novel factors have several unique features that distinguish them from other members in the E2F family. They lack the leucine-zipper domain required for dimerization with partner proteins DP1/2 and instead possess

Table 1. Genotypic Analysis of Embryos during Development

	$E2f7^{+/+}$			$E2f7^{+/-}$			$E2f7^{-/-}$			
	$E2f8^{+/+}$	$E2f8^{+/-}$	$E2f8^{-/-}$	$E2f8^{+/+}$	$E2f8^{+/-}$	$E2f8^{-/-}$	$E2f8^{+/+}$	$E2f8^{+/-}$	$E2f8^{-/-}$	total
E9.5	6	*16*	*29*	16	72(2)	53(1)	12	58(1)	33	299
expected	5	28	22	19	75	56	13	47	34	
E10.5	9	21	13	7(1)	45	28(1)	4(1)	28(1)	6(7)[a]	172
expected	7	20	13	16	43	28	8	23	14	
E11.5	-	*6*	*4*	2	15(2)	14(2)	2(1)	8(1)	0(5)[b]	62
expected	-	5	5	3	16	13	3	10	8	
E12.5	-	-	3	-	4	17(2)	-	3	0(9)[b]	38
expected	-	-	5	-	4	15	-	4	10	
P0	7	22	16	24	45	17	5	18	0[b]	154
expected	8	18	10	18	39	21	10	21	11	

( ), Number of dead embryos recovered. Exact binomial test used to determine significance.
[a] Significant ($p = 0.0015$).
[b] Highly significant ($p < 0.0007$).

two DNA-binding domains that are predicted to interact with each other and foster DP-independent DNA-binding activity. The expression of E2F7 and E2F8 during the cell cycle is also different from that of other E2Fs, with peak levels found later in the cell cycle during S-G_2. Moreover, their overexpression in fibroblasts can, unlike that of other E2Fs, repress E2F-target gene expression and block cell proliferation (de Bruin et al., 2003; Di Stefano et al., 2003; Maiti et al., 2005), suggesting a role for these two E2Fs in facilitating cell cycle transitions. Here, we utilized homologous recombination strategies to inactivate *E2f7* and *E2f8* in mice and rigorously investigate their functions in vivo. From these studies, we conclude that *E2f7*and *E2f8* represent a unique repressive arm of the E2F transcriptional network that is critical for embryonic development and cell survival.

RESULTS

E2F7 and E2F8 Are Essential for Embryonic Viability

To investigate E2F7 and E2F8 function in vivo, we utilized homologous recombination techniques and cre-*loxP* technology to disrupt *E2f7* and *E2f8* function in mice. Targeting the inactivation of *E2f7* and *E2f8* was achieved by flanking exon 4 of *E2f7* and exons 3 and 4 of *E2f8* with *loxP* sites (Figure 1A). Cre-mediated recombination of *loxP*-flanked sequences resulted in the ablation of domains required for DNA binding and in a shift of the open reading frames, leading to premature termination of translation. Pups lacking the *neo* cassette (conditional knockout allele: $E2f7^{loxP}$ or $E2f8^{loxP}$; Figure 1A) or lacking both the *neo* cassette and the *loxP*-flanked regions of *E2f7* or *E2f8* (conventional knockout allele: $E2f7^{-}$ or $E2f8^{-}$; Figure 1A) were identified by Southern blot and PCR genotyping analysis (Figure 1B and data not shown).

To investigate the requirement for these E2Fs in development, we interbred $E2f7^{+/-}$ or $E2f8^{+/-}$ animals and found that $E2f7^{-/-}$ or $E2f8^{-/-}$ pups were born. Mutant pups developed normally through puberty and lived to old age (data not shown). Real-time RT-PCR analysis of gene expression revealed that *E2f7* and *E2f8* mRNA levels were unperturbed in $E2f8^{-/-}$ and $E2f7^{-/-}$ embryos, respectively (Figure 1C), indicating that the absence of abnormalities in single knockout animals is not due to simple compensation at the expression level. We then explored functional redundancy between E2F7 and E2F8 by examining the biological consequence of ablating both simultaneously. To this end, we intercrossed $E2f7^{+/-}E2f8^{+/-}$ animals and analyzed the resulting offspring. Whereas $E2f7^{-/-}E2f8^{+/-}$ and $E2f7^{+/-}E2f8^{-/-}$ pups were born at the expected Mendelian ratios, no $E2f7^{-/-}E2f8^{-/-}$ double knockout (DKO) pups were found in newborn litters (P0) (Table 1). This demonstrates that at least one allele of *E2f7* or *E2f8* is required for embryonic development and viability. The contribution of E2F7 and E2F8 toward postnatal development, however, does not appear to be equal. Young and adult $E2f7^{+/-}E2f8^{-/-}$ mice were developmentally normal, whereas most $E2f7^{-/-}E2f8^{+/-}$ animals appeared runted (Figure 2A) and died within the first 3 months of life (Figure 2B; P90, $p < 0.001$).

Genetic Ablation of *E2f7* and *E2f8* In Vivo Induces Massive Apoptosis in Embryos

Analysis at earlier stages of embryonic development showed that all DKO embryos had a beating heart at embryonic day 9.5 (E9.5). These embryos were noticeably smaller than wild-type littermates (Table 1 and Figure 2C, top panels), but macroscopic inspection did not reveal other obvious defects. By E10.5, only 46% of DKO embryos were alive ($p = 0.0015$) and by E11.5 all DKO embryos were dead ($p < 0.0007$). Live E10.5 embryos often had vascular defects in the yolk sac and in the embryo proper, which were characterized by large dilated blood vessels associated with multifocal hemorrhages (Figure 2C, bottom panels). Other phenotypes were also manifested in tissues distinct from the vasculature. Specifically, multiple areas within the head mesenchyme, branchial arch, somites, and neural tube of DKO fetuses contained cells with pyknotic nuclei surrounded by bright eosinophilic cytoplasm (see Figure S1A in the Supplemental Data available with this article online; data not shown).

These latter observations prompted us to examine proliferation and apoptosis in $E2f7^{-/-}E2f8^{-/-}$ embryos more closely. Since a significant fraction of DKO embryos died by E10.5, proliferation and apoptosis were measured in E9.5 embryos. When assessed by immunohistochemistry using BrdU-specific

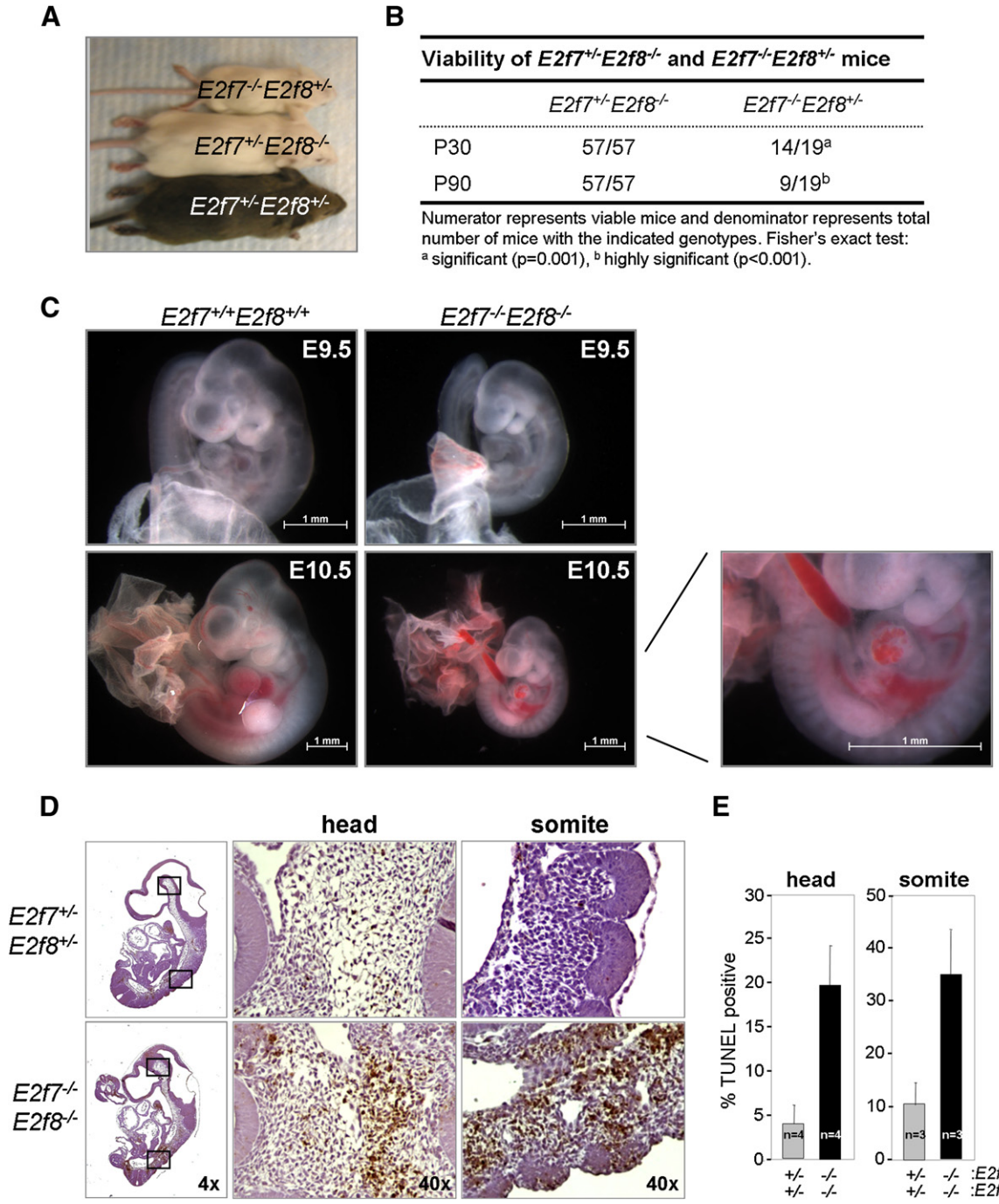

Figure 2. Global Deletion of *E2f7* and *E2f8* Results in Developmental Delay, Vascular Defects, and Widespread Apoptosis In Vivo

(A) Micrograph of $E2f7^{+/-}E2f8^{+/-}$, $E2f7^{+/-}E2f8^{-/-}$, and $E2f7^{-/-}E2f8^{+/-}$ mice at 21 days of age.

(B) Tabulated number of $E2f7^{+/-}E2f8^{-/-}$ and $E2f7^{-/-}E2f8^{+/-}$ mice that live until 30 (P30) and 90 (P90) days of age.

(C) Gross pictures of *E2f7* and *E2f8* double knockout embryos at E9.5 (top panels) and E10.5 (bottom panels). The right panel is a higher magnification view of the vascular defects in E10.5 $E2f7^{-/-}E2f8^{-/-}$ embryos.

(D) E9.5 embryos with the indicated genotypes were analyzed by TUNEL assays. Far left panels: low magnification pictures of whole embryos. Right two panels: high magnification images of representative areas demarcated by the box in the low magnification images.

(E) Quantification of TUNEL-positive cells in the indicated tissue areas are presented as the average ± SD percentage (%) of cells that are TUNEL positive. Three sections per embryo and at least three different embryos for each genotype were analyzed.

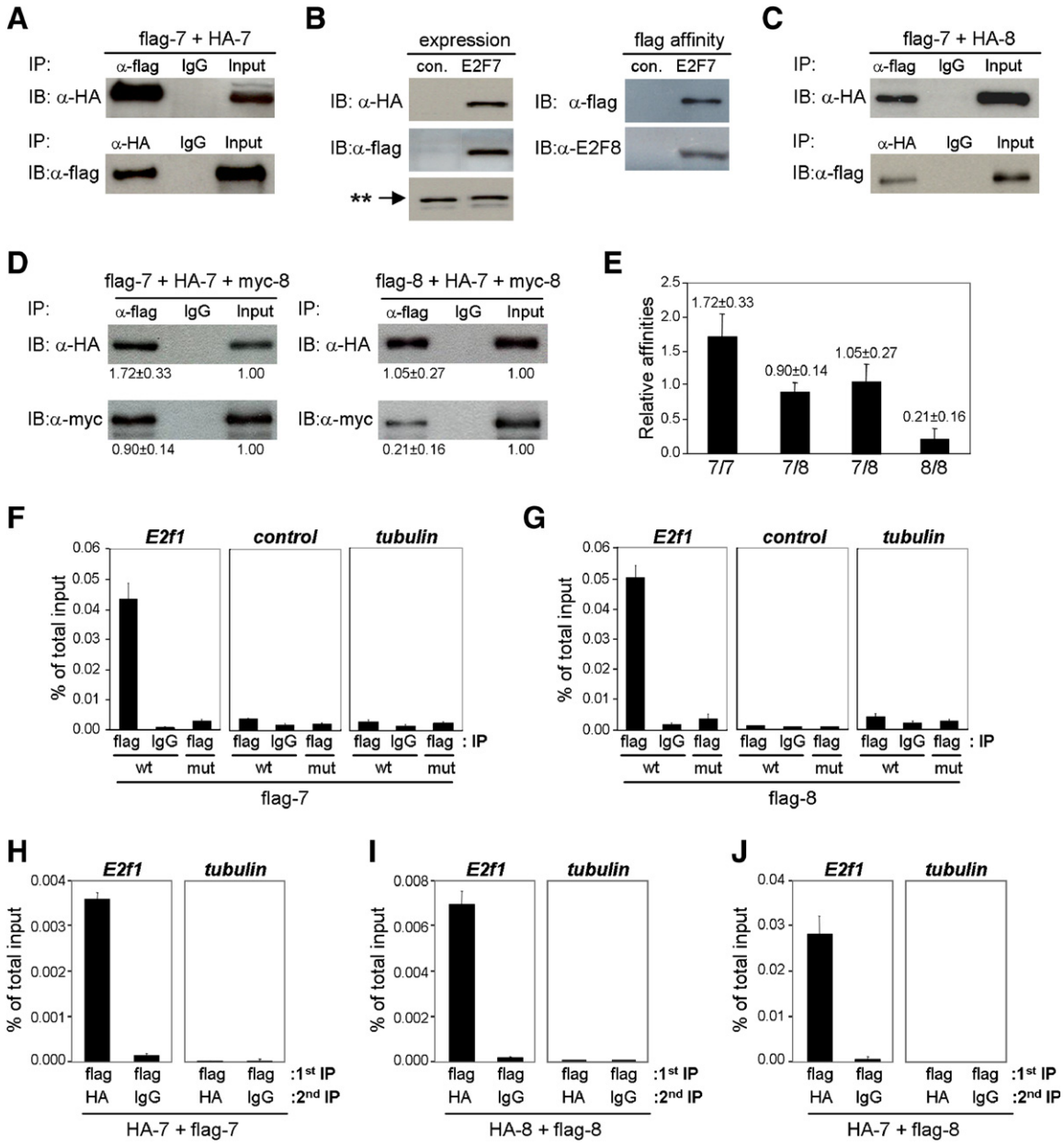

Figure 3. E2F7 and E2F8 Homo- and Heterodimerize

(A) Homodimerization of E2F7. Lysates from cells transfected with both flag-tagged E2F7 (flag-7) and HA-tagged E2F7 (HA-7) were immunoprecipitated (IP) and immunoblotted (IB) with anti-flag and anti-HA antibodies as indicated. Immunoprecipitation with normal mouse IgG was used as a negative control.

(B) Left panels: stable expression of flag-HA-E2F7 in HeLa cells. Flag-HA-E2F7 transduced HeLa cell lysates were subjected to western blotting. The presence of a nonspecific protein indicated by (**) was used as a loading control. Right panels: Endogenous E2F8 associates with flag-HA-E2F7. Nuclear extracts from flag-HA-E2F7-expressing cells were immunoprecipitated with flag antibody affinity resins as described in Experimental Procedures, and eluents were immunoblotted with E2F8-specific antibodies. Mock-transduced HeLa cells (con.) were used as a negative control.

(C) Heterodimerization of E2F7 and E2F8. Lysates derived from cells overexpressing both flag-E2F7 and HA-E2F8 were immunoprecipitated (IP) with anti-flag antibodies and immunoblotted (IB) with anti-HA antibodies (top panel) or vice versa (bottom panel). Immunoprecipitation with normal mouse IgG was used as a negative control.

(D) Kinetic analysis of dimerization. HEK293 cells overexpressing the indicated constructs were subjected to anti-flag immunoprecipitation (IP), followed by anti-HA or anti-myc immunoblotting (IB) as indicated. The amount of detected E2F7 and E2F8 was measured by densitometry and quantified relative to 1% of the input material. The relative levels indicated at the bottom of each lane are presented as the average ± SD of three independent experiments where input is always equal to 1.00.

(E) Bar graph presentation of the kinetic analysis of dimerization shown in (D).

(F) E2F7 binds to the *E2f1* promoter. Chromatin from cells overexpressing wild-type flag-E2F7 (wt) or flag-E2F7DBD1,2 (mut) was immunoprecipitated (IP) with anti-flag or IgG control antibodies. Immunoprecipitated DNA was amplified using primers specific for the *E2f1* promoter (*E2f1*), irrelevant sequences in exon 1 of *E2f1*, and the *tubulin* promoter (*control* and *tubulin,* respectively).

antibodies, we observed no detectable difference in the percentage of cells incorporating BrdU between wild-type and DKO embryos (Figure S2). We did observe, however, a marked increase in cells labeled by TdT-mediated dUTP nick end-labeling (TUNEL) in areas of DKO embryos previously noted to contain abundant pyknotic nuclei, confirming widespread apoptosis in these tissues (Figures 2D and 2E, Figures S1B and S1C). In summary, global deletion of *E2f7* and *E2f8* resulted in a spectrum of embryonic defects impacting the vasculature and cell survival.

E2F7 and E2F8 Form Homodimers and Heterodimers

Previous studies suggested that E2F7 and E2F8 form homodimers (Di Stefano et al., 2003; Logan et al., 2004; Maiti et al., 2005). Coimmunoprecipitation (CoIP) assays using HEK293 cells coexpressing flag-tagged and HA-tagged versions of E2F7 or E2F8 confirmed their ability to form homodimers (Figure 3A and data not shown). Given that E2F7 and E2F8 are coexpressed in most tissues of the embryo (Figure 1D), we also explored the possibility that E2F7 may physically interact with E2F8. Because immunoprecipitation-quality antibodies for E2F7 and E2F8 are not yet available, we assessed the ability of flag-tagged E2F7 to complex with endogenous E2F8 and vice versa. As shown in Figure 3B (and data not shown), these immunoaffinity purification assays revealed an association between E2F7 and E2F8. Heterodimerization was confirmed by CoIP assays using HEK293 cells coexpressing flag-E2F7 and HA-E2F8 (Figure 3C).

Given the redundant functions of E2F7 and E2F8 in development, we evaluated their preferred dimerization state in cells. To this end, HEK293 cells were cotransfected with flag-E2F7, HA-E2F7, and myc-E2F8, or alternatively with flag-E2F8, HA-E2F7, and myc-E2F8. We then measured the relative amounts of homo- versus heterodimers by immunoprecipitation with flag-antibodies followed by immunoblotting with either HA- or myc-antibodies; the amount of E2F7 and E2F8 on blots was normalized to 1% of the input material. Quantification of three independent experiments showed that E2F7 had a greater binding affinity to itself than to E2F8 (Figures 3D and 3E). On the other hand, E2F8 had a greater binding affinity for E2F7 than for itself. From this analysis we conclude that, at least in cultured cells, the preferred state of dimerization is E2F7:E2F7 > E2F7:E2F8 > E2F8:E2F8.

E2f1 Is a Direct Target of E2F7 and E2F8

We then utilized chromatin immunoprecipitation (ChIP) assays to assess the ability of E2F7 and E2F8 to bind known E2F target promoters. Quantitative real-time PCR assays showed that flag-tagged versions of E2F7 and E2F8 were recruited to E2F-binding sites present on the *E2f1* and *cdc6* promoters but not to irrelevant sequences in these genes (exons 1) or the *tubulin* promoter (Figures 3F and 3G, Figures S4A and S4B, and data not shown). This recruitment was specific since IgG failed to immunoprecipitate target-promoter sequences. Moreover, anti-flag antibodies failed to immunoprecipitate target promoters from cell lysates expressing mutant forms of E2F7 or E2F8 that are incapable of binding DNA.

We then used sequential ChIP techniques to address whether E2F7 and E2F8 could be recruited to the target promoters as homo- and heterodimers. To this end, HEK293 cells expressing various combinations of HA-tagged and flag-tagged versions of E2F7 and E2F8 were first immunoprecipitated with anti-flag antibodies. Immunoprecipitated DNA-protein complexes were then eluted with excess flag peptide and reimmunoprecipitated with HA-specific antibodies. The final immunoprecipitates were amplified with primers specific for the *E2f1, cdc6*, or *tubulin* promoters as described above (Figures 3H–3J, Figures S4C–S4E). These sequential ChIP assays showed that both homo- and heterodimers of E2F7 and E2F8 could occupy E2F-binding sites on E2F-target promoters, including *E2f1*.

E2f1 Expression Is Derepressed in $E2f7^{-/-}E2f8^{-/-}$ MEFs

To determine whether the recruitment of E2F7 and E2F8 to the target promoters had any functional consequence on its expression, we initially examined E2F1 protein and mRNA levels in mouse embryo fibroblasts (MEFs) deficient for both *E2f7* and *E2f8*. Because $E2f7^{-/-}E2f8^{-/-}$ embryos died early during mouse development, we derived MEFs from E13.5 $E2f7^{loxP/loxP}$ $E2f8^{loxP/loxP}$ embryos and then ablated *E2f7* and *E2f8* expression in vitro using a *cre* recombinase-expressing retrovirus. PCR genotyping of genomic DNA and real-time RT-PCR analysis of *E2f7* and *E2f8* expression confirmed their efficient deletion (Figure 4A). These experiments showed that DKO cells have higher E2F1 protein and mRNA levels than control-treated MEFs (Figures 4B and 4C, respectively). Interestingly, there was also an increase of p53 protein in DKO MEFs, consistent with the ability of E2F1 to induce the accumulation of p53 (Hsieh et al., 2002; Pomerantz et al., 1998; Rogoff et al., 2002; Russell et al., 2002). Introduction of an *E2f1* luciferase promoter construct into wild-type and DKO MEFs revealed higher luciferase reporter activity in DKO cells (Figure 4D), indicating that the higher levels of E2F1 mRNA and protein in DKO MEFs are likely due to transcriptional deregulation. Together with the ChIP assays shown in Figures 3F–3J, these data suggest that the repression of *E2f1* by E2F7 and E2F8 is direct.

To examine whether E2F7- and E2F8-mediated repression might be cell cycle dependent, we compared E2F-target expression in synchronized populations of wild-type and DKO MEFs stimulated to progress through the cell cycle. MEFs were synchronized in G_1/S by serum deprivation followed by restimulation with medium containing 15% serum and 1 mM hydroxyurea

(G) E2F8 binds to the *E2f1* promoter. Cells overexpressing wild-type flag-E2F8 (wt) or flag-E2F8DBD1,2 (mut) was immunoprecipitated (IP) with anti-flag or normal mouse IgG antibodies. Immunoprecipitated DNA was amplified using primers specific for the *E2f1* promoter (*E2f1*), exon 1 of *E2f1* (*control*), and the *tubulin* promoter (*tubulin*).

(H–J) Homodimers and heterodimers of E2F7 and E2F8 occupy the *E2f1* promoter. Cell extracts expressing ectopic HA-E2F7 and flag-E2F7 (H), HA-E2F8 and flag-E2F8 (I), HA-E2F7 and flag-E2F8 (J) were used for sequential ChIP assays as described in Experimental Procedures. Antibodies used for the first and second round of immunoprecipitation are indicated (1^{st} IP and 2^{nd} IP, respectively). Immunoprecipitated DNA collected after two rounds of ChIP was amplified using primers specific for the *E2f1* promoter (*E2f1*) or for the *tubulin* promoter (*tubulin*). For all the ChIP experiments, real-time PCR cycle numbers were normalized to 1% of the input DNA. Data are presented as the average ± SD percentage (%) of total input in samples analyzed in triplicate.

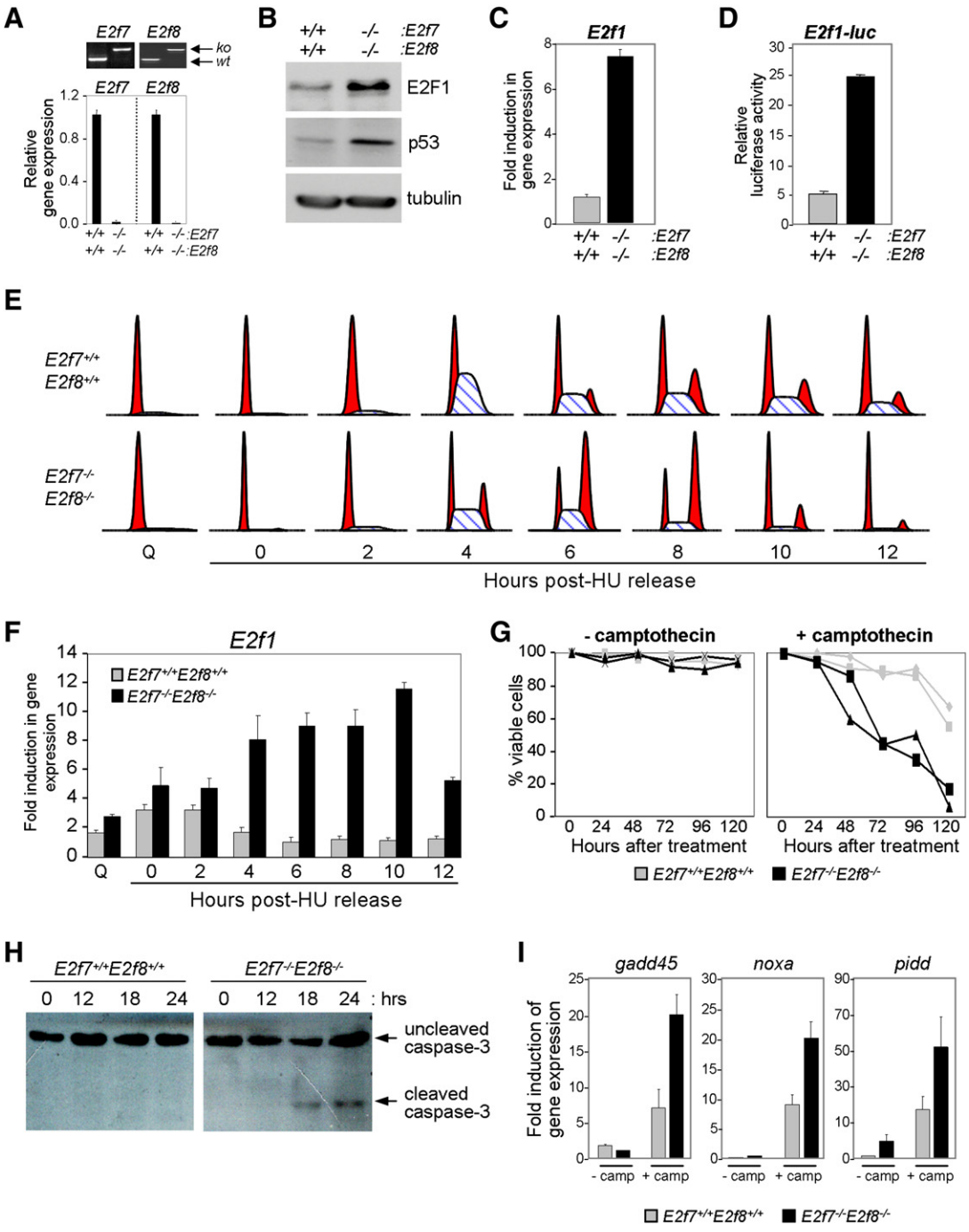

Figure 4. Loss of E2F7 and E2F8 Results in an Increase of E2F1 and p53 Proteins and Sensitizes MEFs to Apoptosis

(A–F) Deregulation of *E2f1* and *p53* expression in MEFs deficient in *E2f7* and *E2f8*.

(A) Top panels: PCR genotyping analysis of DNA isolated from $E2f7^{+/+}E2f8^{+/+}$ and $E2f7^{loxP/loxP}E2f8^{loxP/loxP}$ MEFs treated with *cre*-expressing retroviruses. The knockout (*ko*) and wild-type (*wt*) alleles are indicated. Bottom graphs: Real-time RT-PCR analysis of *E2f7* and *E2f8* expression in cells. For convenience, cre-deleted *loxP* alleles were labeled as (−/−) at bottom of graphs.

(B) Western blot analysis of lysates described in (A) using antibodies specific for E2F1 and p53 as indicated. Tubulin-specific antibodies were used as an internal loading control.

(C) Expression of *E2f1* in MEFs treated as in (A) was measured by real-time RT-PCR.

(D) Cells treated as in (A) were cotransfected with the *E2f1* firefly luciferase and thymidine kinase renilla luciferase reporter plasmids (internal control). Relative *E2f1-luc* reporter activity was normalized to renilla luciferase activity. A representative of at least three independent experiments is shown. Data are presented as the average ± SD from samples analyzed in triplicate.

(HU). Cells were then washed and incubated with medium lacking HU and harvested at various times following HU release. Cell cycle progression was monitored by flow cytometry (Figure 4E). As expected, the expression of *E2f1* and *cdc6* in wild-type cells peaked at G_1/S and subsequently decreased as cells entered S phase and progressed through G_2 (Figure 4F, Figure S5A). Strikingly, expression of *E2f1* and *cdc6* in DKO cells continued to increase during S and G_2, accumulating up to 12-fold higher levels than in wild-type cells. These data suggest an important role for E2F7- and E2F8-mediated repression during S and G_2, coinciding with the time of the cell cycle when these two E2Fs accumulate maximally (de Bruin et al., 2003; Maiti et al., 2005).

DKO Cells Are Hypersensitive to DNA Damage

Given the marked increase in the expression of multiple E2F-target genes in cells deficient for *E2f7* and *E2f8*, we analyzed proliferation rates in these double-mutant cells. These analyses failed to reveal any significant difference in the proliferation of DKO and wild-type cells (Figure S5B and data not shown), even though DKO cells appeared to transit through S phase 2–3 hr faster than control cells (Figure 4E). Presumably, faster progression through S phase was compensated by a concomitant delay in other phases of the cell cycle as previously reported for cells lacking *Rb* or overexpressing *dE2f1* (Resnitzky et al., 1994; Reis and Edgar, 2004). Because overexpression of *E2f1* has been shown to elicit apoptosis in cells treated with DNA-damage-inducing agents (Stevens and La Thangue, 2004), we tested the sensitivity of DKO cells to camptothecin and cisplatin, two DNA-damage-inducing drugs. To this end, asynchronously proliferating wild-type and DKO MEFs were treated with camptothecin or cisplatin and cell viability was determined by trypan blue exclusion. These drugs induced a significant acceleration of cell death in DKO MEFs when compared to wild-type MEFs (Figure 4G and data not shown). Drug-treated DKO cells detached from tissue culture plates and exhibited the characteristic blebbing morphology of apoptotic cells (Figure S5C). Consistent with this observation, drug treatment preferentially triggered cleavage of caspase-3 in DKO MEFs (Figure 4H). We also evaluated the levels of E2F1 and p53 in drug-treated DKO MEFs. As expected, E2F1 and p53 protein levels accumulated to higher levels in camptothecin-treated DKO cells than in similarly treated wild-type cells (Figure S5D). The increase in p53 protein corresponded with a marked increase in the expression of p53-responsive genes, including *gadd45*, *noxa*, and *pidd* (Figure 4I). These results suggest that E2F7 and E2F8 may attenuate DNA-damage-induced apoptosis by preventing the aberrant accumulation of E2F1 and p53.

Induction of Apoptosis in *E2f7*$^{-/-}$*E2f8*$^{-/-}$ Embryos Is Dependent on E2F1 and p53

Given the above observations, we hypothesized that the apoptosis in *E2f7*$^{-/-}$*E2f8*$^{-/-}$ embryos might be mediated through the induction of E2F1 and/or p53. To test this possibility, *E2f7*$^{+/-}$*E2f8*$^{-/-}$ animals were bred with either *E2f1*$^{-/-}$ or *p53*$^{-/-}$ animals in order to generate cohorts of triple knockout embryos (TKO). TUNEL assays performed on E9.5 TKO embryos showed that the loss of either *E2f1* or *p53* suppressed the massive apoptosis caused by a deficiency in *E2f7* and *E2f8* (Figures 5A and 5B). From these results, we conclude that E2F7 and E2F8 represent a critical regulatory arm of the E2F network that controls apoptosis through the E2F1-p53 axis.

Interestingly, both cohorts of TKO embryos harvested at E10.5 had dilated vessels and extensive hemorrhaging similar to DKO embryos (data not shown). Importantly, no live TKO embryos could be observed at E12.5 (Figures 5C and 5D). These results suggest that the widespread apoptosis observed in DKO embryos, which was suppressed in TKO embryos, is independent of vascular defects and embryonic lethality. These results also indicate that misregulated E2F7- and E2F8-target genes beyond *E2f1* are likely to be involved in the mortality of DKO embryos.

Consistent with this view, global analysis of gene expression showed that among the ~39,000 transcripts analyzed, 88 were upregulated and 33 were downregulated at least 3-fold in *E2f7*$^{-/-}$*E2f8*$^{-/-}$ embryos relative to wild-type embryos (Figure 6A). Real-time RT-PCR assays confirmed the altered expression of many of these genes (Figure 6B). Functional annotation of misregulated genes revealed a bias for gene products known to be activated in response to stresses, including hypoxia, nutrient deprivation, and apoptosis (Figure 6C and Figure S6). These analyses also confirmed that *E2f1*, *cdc6*, and additional E2F targets were increased in DKO versus wild-type embryos, albeit the increase in their expression was only ~2-fold (data not shown). Interestingly, a subset of the 122 transcripts (88 up- and 33 downregulated) were partially misregulated in *E2f7*$^{-/-}$, *E2f8*$^{-/-}$, and/or *E2f7*$^{+/-}$*E2f8*$^{+/-}$ embryos, underscoring the synergistic role of these two E2F factors in the control of gene expression during embryonic development.

DISCUSSION

The E2F7 and E2F8 transcription factors likely represent the final members of the E2F family to be identified in mammals. We show here that these two novel factors are strictly required for embryonic development and are critical direct regulators of the E2F1-p53 apoptotic axis.

(E) FACS analysis of synchronized cre-treated *E2f7*$^{+/+}$*E2f8*$^{+/+}$ and *E2f7*$^{loxP/loxP}$*E2f8*$^{loxP/loxP}$ MEFs. For convenience, cre-deleted *loxP* alleles were labeled as (−/−). MEFs were synchronized by serum deprivation and hydroxyurea (HU) block as described in Experimental Procedures. At the indicated time points, cells were harvested and stained by propidium iodide for flow cytometry. Q, quiescent cells kept in serum-deprived medium.

(F) Total RNA isolated from same synchronized MEFs samples as in (E) was analyzed by real-time RT-PCR assays specific for *E2f1* expression.

(G–I) MEFs deficient in *E2f7* and *E2f8* are hypersensitive to DNA-damage-induced apoptosis.

(G) Cre-treated *E2f7*$^{+/+}$*E2f8*$^{+/+}$ and *E2f7*$^{loxP/loxP}$*E2f8*$^{loxP/loxP}$ MEFs were mock treated with DMSO (−camptothecin) or with camptothecin (+camptothecin). At the indicated intervals, cells were harvested and counted in triplicate as described in Experimental Procedures. The average ± SD percentages (%) of viable cells at the indicated time points are presented.

(H) Lysates derived from MEFs treated as in (G) were analyzed at indicated time points by western blotting using caspase-3-specific antibodies.

(I) Total RNA was extracted from cells treated for 18 hr as in (G), and expression of the indicated p53 target genes was measured by real-time RT-PCR. For all the real-time PCR experiments, samples with the lowest expression were normalized to 1. Data are presented as the average ± SD-fold induction in samples analyzed in triplicate.

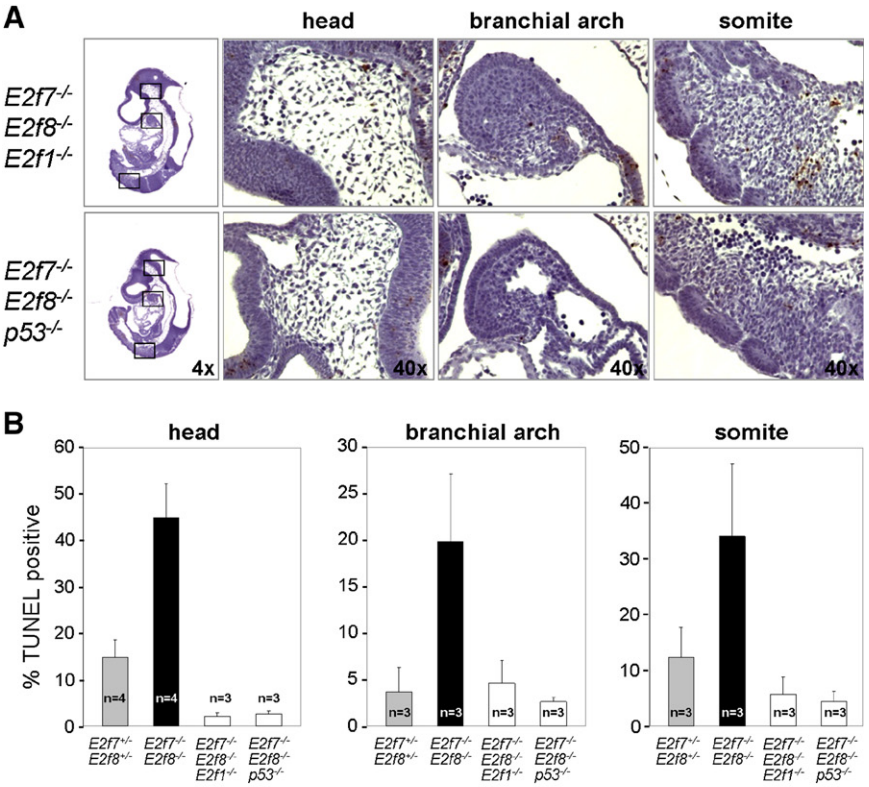

Figure 5. Loss of *E2f1* or *p53* Suppresses Apoptosis in $E2f7^{-/-}E2f8^{-/-}$ Embryos

(A) Micrographs of TUNEL-stained E9.5 $E2f7^{-/-}E2f8^{-/-}E2f1^{-/-}$ (top panels) and $E2f7^{-/-}E2f8^{-/-}p53^{-/-}$ embryos (bottom panels). Far left panels: low magnification pictures of whole embryos. Right three panels: high magnification images of representative areas demarcated by the box in the low magnification images.

(B) Quantification of TUNEL-positive cells in the indicated tissue areas is presented as the average ± SD percentage (%) of cells that are TUNEL positive. Three sections per embryo and at least three different embryos for each genotype were analyzed. For comparison purposes, data derived from $E2f7^{+/-}E2f8^{+/-}$ and $E2f7^{-/-}E2f8^{-/-}$ in Figure 2E and Figure S1C were included.

(C) Genotypic analysis of embryos derived from $E2f1^{+/-}E2f7^{+/-}E2f8^{-/-}$ intercrosses at the indicated stages of development.

(D) Genotypic analysis of embryos derived from $p53^{+/-}E2f7^{+/-}E2f8^{-/-}$ intercrosses at the indicated stages of development.

C

Genotypic analysis of embryos during development

	$E2f1^{+/+}$ / $E2f7^{-/-}E2f8^{-/-}$	$E2f1^{+/-}$ / $E2f7^{-/-}E2f8^{-/-}$	$E2f1^{-/-}$ / $E2f7^{-/-}E2f8^{-/-}$	total
E9.5	-	2	5	46
expected	-	*5*	*6*	
E12.5	-	-	0(4)[a]	10
expected	-	-	*3*	

() number of dead embryos; Exact binomial test: [a] highly significant (p<0.0007)

D

Genotypic analysis of embryos during development

	$p53^{+/+}$ / $E2f7^{-/-}E2f8^{-/-}$	$p53^{+/-}$ / $E2f7^{-/-}E2f8^{-/-}$	$p53^{-/-}$ / $E2f7^{-/-}E2f8^{-/-}$	total
E9.5	3	6	4	66
expected	*4*	*8*	*4*	
E12.5	0	0(1)	0(4)[a]	12
expected	*1*	*2*	*1*	

() number of dead embryos; Exact binomial test: [a] highly significant (p<0.0007).

While disruption of *E2f7* or *E2f8* had little impact on mouse development, their combined ablation resulted in widespread apoptosis, vascular defects, and hemorrhaging, leading to embryonic death by E11.5. Provision of even one functional allele from either locus was sufficient to carry fetuses through development all the way to birth. The contribution of E2F7 and E2F8 in postnatal development, however, does not appear to be equal. Young and adult $E2f7^{+/-}E2f8^{-/-}$ mice were developmentally normal, whereas most $E2f7^{-/-}E2f8^{+/-}$ animals appeared runted and died within the first three months of life. A bias in homo- versus heterodimerization may explain the differential requirement for *E2f7* and *E2f8* in postnatal development. We found that in tissue culture experiments, under conditions where expression levels can be compared (by epitope tagging) and experimentally equalized, the formation of E2F7:E2F7 homodimers was preferred over E2F7:E2F8 heterodimers, and E2F8:E2F8 homodimers appeared to be the least preferred state (E2F7:E2F7 > E2F7:E2F8 > E2F8:E2F8). While the molecular basis for homo- versus heterodimerization is not yet clear, these data suggest that inefficient homodimerization may compromise the ability of E2F8 to compensate for the loss of E2F7, an effect that might be aggravated in circumstances of limiting amounts of E2F8 (i.e., $E2f7^{-/-}E2f8^{+/-}$). Thus, the observed bias for E2F7 homodimerization may explain the stricter postnatal requirement for this subunit. While this interpretation is likely an oversimplification, these results do provide a molecular explanation for their functional redundancy in development. It will be interesting to investigate how dimerization might be impacted by the levels of E2F7 and E2F8 proteins in vivo or by tissue-specific signals.

Because of the intense interest in E2Fs as major regulators of the cell cycle and apoptosis, individual E2F family members, including *E2f1* through *E2f6*, have been extensively studied in vivo by gene-targeting approaches in mice. With the exception of *E2f3* knockout mice, defects in embryos deficient for each of

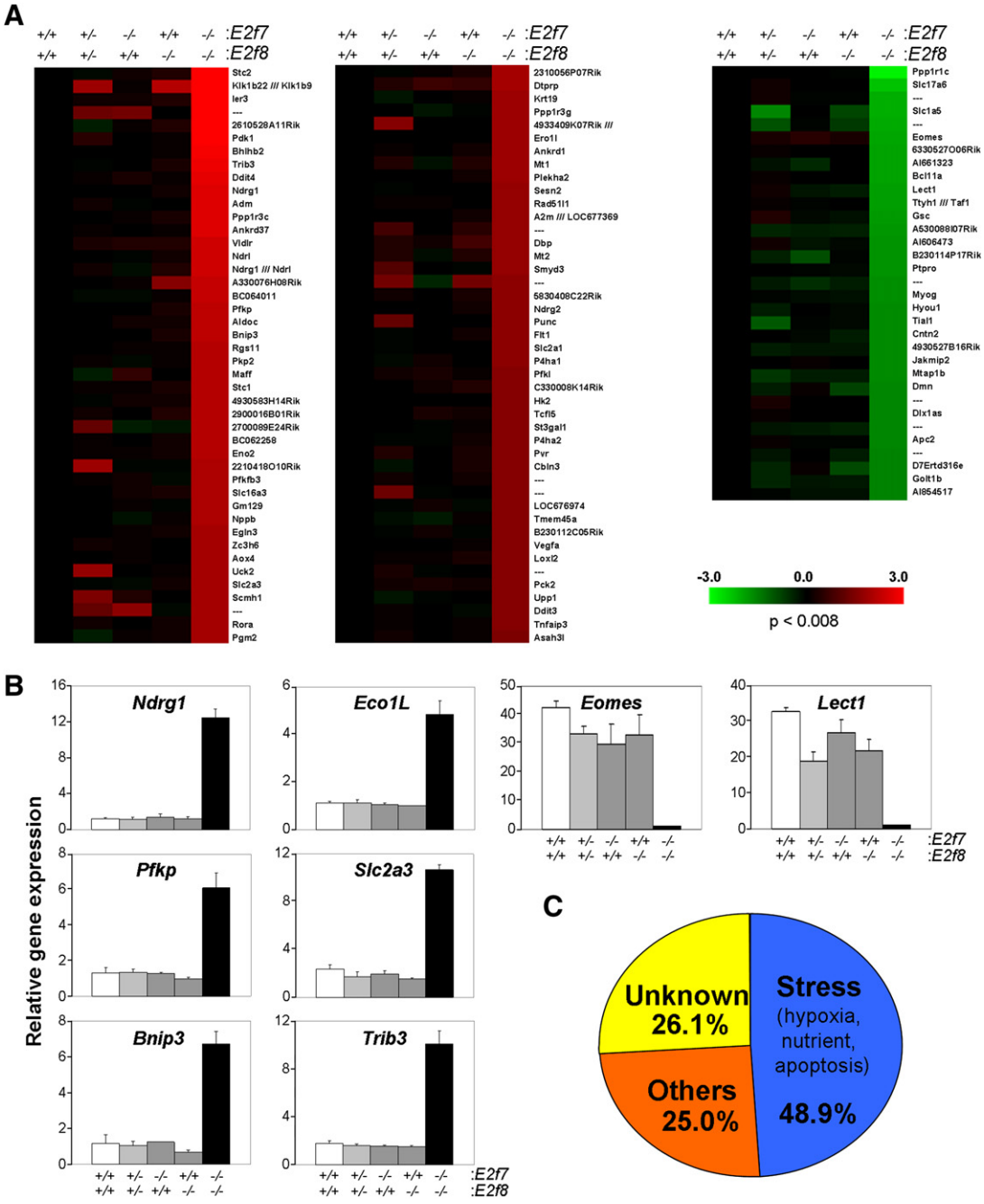

Figure 6. Microarray Analysis of E10.5 Embryos

(A) Heat maps of probe sets in Affymetrix microarrays that showed at least a 3-fold induction (left and middle) or a 3-fold reduction (right) of expression in *E2f7*$^{-/-}$ *E2f8*$^{-/-}$ relative to wild-type embryos. Data are presented as the medium of four embryos from wild-type, *E2f7*$^{-/-}$*E2f8*$^{+/+}$, and *E2f7*$^{+/+}$*E2f8*$^{-/-}$genotype groups, and the medium of two embryos from *E2f7*$^{+/-}$ *E2f8*$^{+/-}$ and *E2f7*$^{-/-}$*E2f8*$^{-/-}$ genotype groups. Red and green indicate induction and reduction, respectively. Probe sets representing genes of interest are indicated.

(B) The expression of eight target genes (six upregulated and two downregulated) was evaluated by real-time RT-PCR assays; samples with lowest expression were normalized to 1. Data are presented as the average ± SD-fold induction in samples analyzed in triplicate.

(C) Pie chart diagram illustrates the over-representation of stress-related genes among the total 88 upregulated genes in DKO embryos.

the known E2Fs are rather subtle (Field et al., 1996; Yamasaki et al., 1996; Lindeman et al., 1998; Humbert et al., 2000a; Murga et al., 2001; Storre et al., 2002; Rempel et al., 2000). Even the disruption of *E2f3* when in a mixed genetic background yields viable mice (Humbert et al., 2000b; Wu et al., 2001). The virtual absence of cell proliferation and apoptotic defects in E2F-deficient

embryos has raised questions about the physiological importance of these factors, leaving the impression that E2Fs must either not be critical for the control of these processes in vivo or that there is sufficient functional redundancy among family members to accommodate for a deficiency in any single member. Previous tissue culture experiments have provided evidence for functional redundancy among E2F1-3 activators and E2F4-6 repressors in the control of proliferation (Gaubatz et al., 2000; Wu et al., 2001; Giangrande et al., 2004). The current work underscores functional redundancy among E2F7 and E2F8 in the control of apoptosis in vivo.

Too much or unrestrained E2F activity can also compromise cell homeostasis. The importance of restraining E2F activity is highlighted by the fact that at least four independent mechanisms have evolved to achieve this. One such repressive mechanism involves the binding and inhibition of E2F proteins by the Rb tumor suppressor. Indeed, disruption of Rb leads to unregulated proliferation and ectopic apoptosis that is partly suppressed by the concomitant loss of E2F activators (Ziebold et al., 2001; Saavedra et al., 2002). A second mechanism involves binding of cyclinA/cdk2 to E2F1, E2F2, and E2F3a proteins during S phase, leading to the phosphorylation of their dimerization partners DP1/2 and the inhibition of E2F/DP DNA-binding activity (Dynlacht et al., 1994). A third mechanism involves the p45SKP2/F-box-dependent degradation of the three E2F activators during S phase (Leone et al., 1998; Marti et al., 1999). Here, we described a fourth repressive mechanism to keep E2F activity in control that involves direct transcriptional repression of *E2f1* by E2F7 and E2F8. In contrast to other repressor E2Fs (E2F3b, E2F4-6), which play a predominant role in silencing gene expression in G_0-G_1, these two novel E2Fs may have a particularly important role in repressing E2F targets as cells transit through S phase and into G_2. Gene expression analysis in synchronized $E2f7^{-/-}E2f8^{-/-}$ MEFs revealed that *E2f1* mRNA levels, as well as those of many other E2F-target genes, increased acutely during S and G_2. Thus, by participating in the repression of E2F-target genes as cells transit through S-G_2, E2F7 and E2F8 represent, to our knowledge, the first transcriptional mechanism described in mammals that contributes directly to the downswing in the oscillating pattern of cell-cycle-specific gene expression.

In vitro and in vivo experiments described here provide clear-cut evidence for a role of E2F7 and E2F8 in the control of apoptosis that involves, at least in part, the regulation of *E2f1* expression. Genetic inactivation of *E2f7* and *E2f8* resulted in the accumulation of *E2f1* mRNA and a corresponding increase in its protein product. Consistent with a direct role in repression, ChIP experiments showed that E2F7 and E2F8 are recruited to the *E2f1* promoter and that this requires intact DNA-binding activity. The increase of E2F1 protein levels in $E2f7^{-/-}E2f8^{-/-}$ cells coincided with the accumulation of p53 protein. Several mechanisms of how E2F1 may lead to the accumulation and activation of p53 have been described (Hsieh et al., 2002; Pomerantz et al., 1998; Rogoff et al., 2002; Russell et al., 2002). The increase of E2F1 and p53 in $E2f7^{-/-}E2f8^{-/-}$ cells is of physiological significance since ablation of either *E2f1* or *p53* suppressed the widespread apoptosis observed in DKO embryos. The fact that these TKO embryos still died suggests that apoptosis in $E2f7^{-/-}E2f8^{-/-}$ embryos is not simply due to an indirect consequence associated with embryonic lethality but rather due to a specific signal emanating from deregulated E2F1. These results also indicate that additional targets repressed by E2F7 and E2F8 must be involved in the many pathologies that likely underlie the lethality of DKO embryos. Indeed, profiling of global gene expression in DKO embryos confirmed the deregulation of many additional genes. Interestingly, a substantial portion of these included gene products known to be involved in various responses to stress such as hypoxia, nutrient deprivation, and apoptosis. We view these results to mean that physiological stress, whether induced by vascular or other defects in DKO embryos or by the addition of DNA-damaging agents in DKO MEFs, exacerbates the activation of the E2F1-p53 axis and unleashes a massive apoptotic response.

In summary, we show that E2F7 and E2F8 are essential for embryonic development. Their synergistic function may be viewed as a distinct arm of the E2F network involved in repression of transcription during S-G_2, where *E2f1* represents a particularly critical target that if not appropriately repressed can illicit widespread apoptosis in developing embryos.

EXPERIMENTAL PROCEDURES

Generation of *E2f7* and *E2f8* Knockout Mice

E2f7- and *E2f8*-specific probes were used to screen a 129Sv/Ev bacterial artificial chromosome library. A 7.0 kb *XbaI* fragment of *E2f7* spanning exon 4 and 5 was isolated from *RPCI 22 431 H17*, and a 6.6 kb fragment of *E2f8* containing exon 3 and 4 was isolated from *RPCI 22 539 P23.* Standard cloning techniques were used to generate *E2f7*- and *E2f8*-targeting vectors, which were confirmed by direct sequencing. Targeting vectors were linearized with *NotI* and electroporated into TC1 129Sv/Ev embryonic stem (ES) cells. ES cells were selected in medium containing G418 plus ganciclovir, and correct recombination was confirmed by Southern blots using the indicated probes in Figure 1A. Selected ES clones were injected into C57BL/6 blastocysts to generate chimeric mice, which were bred with Black Swiss females to obtain germline transmission. Appropriate offspring were then bred to *Ella-Cre* mice (Lakso et al., 1996) to produce mice with conventional and conditional null alleles as illustrated in Figure 1A. Genotypic analysis of offspring was performed by Southern blot analysis and multiplex PCR using allele-specific primers described in Figure S7.

Real-Time RT-PCR

Total RNA was isolated using QIAGEN RNA miniprep columns as described by the manufacturer, which included the optional DNase treatment before elution from columns. Reverse transcription of total RNA was performed using Superscript III reverse transcriptase (Invitrogen) and RNase Inhibitor (Roche) according to the manufacturer's protocol. Real-time PCR was performed using a BioRad iCycler, reactions were performed in triplicate, and relative amounts of cDNA were normalized to GAPDH. The *E2f7* and *E2f8* real-time primers are located within the deleted regions of *E2f7* and *E2f8*, respectively. Primer sequences for the indicated genes are included in Figure S7.

Whole-Mount In Situ Hybridization

Wild-type E9.5 day-old embryos were harvested and fixed in 4% paraformaldehyde. Whole mounts were performed as described (Riddle et al., 1993). Probes for *E2f7* and *E2f8* were generated by PCR amplification (see Figure S7). The resulting PCR products were subcloned into pBluescript KS (Stratagene) and pGEM-TEasy vector (Promega), respectively. Sense and antisense RNA probes were transcribed from the appropriate promoters using T3 and T7 RNA polymerase (Roche).

Affimetrix Microarray Analysis

Total RNA was prepared from E10.5 embryos using the RNasy Kit (QIAGEN) and included the optional DNase treatment before elution from purification columns. RNA was processed as described in http://www.osuccc.osu.edu/microarray and hybridized to oligonucleotide microarrays (Mouse Genome 430 2.0 array, Affymetrix, Santa Clara, CA). Scanned image files were quantified with GENECHIP 3.2 (Affymetrix). The Raw gene expression data is presented in Figure S8. Genes that increased or decreased at least 3-fold ($p < 0.008$) in DKO samples relative to wild-type samples were used to generate the heatmaps illustrated in Figure 6A.

Coimmunoprecipitation Assays

Human embryonic kidney (HEK) 293 cells were cultured in DMEM medium supplemented with 15% FBS and used for coimmunoprecipitation assays (CoIP). Transient transfections with the indicated constructs were performed by standard calcium chloride techniques. Cells were harvested and washed in PBS at 4°C, and cell pellets were lysed in 10 volumes of lysis buffer (0.05 M sodium phosphate [pH 7.3], 0.3 M NaCl, 0.1% NP40, 10% glycerol with protease inhibitor cocktail, Roche). CoIP was performed as described before (Maiti et al., 2005).

Immunoaffinity Purification

HeLa cells were transduced with retroviruses expressing a bicistronic mRNA encoding human E2F7 or E2F8 (flag-HA-7 and flag-HA-8) and interleukin-2 receptor (IL-2R)-α (Ogawa et al., 2002). The transduced population was incubated with magnetic beads linked to IL-2R-specific antibodies. E2F7/8-IL-2R-expressing cells were then enriched by separating magnetic beads-bound cells from non-bound cells using a magnetic plate. Nuclear extracts from enriched E2F7/8-expressing cells were prepared by a modified Dignam preparation protocol using Buffer C-450 (20 mM HEPES [pH 7.9], 450 mM KCl, 1.5 mM $MgCl_2$, 25% glycerol, and 0.2 mM EDTA) (Dignam et al., 1983). Resulting extracts were incubated with pre-equilibrated flag M2 affinity resin (A2220, Sigma) for 3 hr. Resin/extract mixtures were decanted onto Bio-Spin columns (BioRad) and allowed to empty by gravity. After extensive washing with Wash Buffer (20 mM HEPES [pH 7.9], 150 mM KCl, 10% glycerol, and 0.2 mM EDTA), complexes were eluted by incubation with 200 μg/ml of flag peptide (F3290, Sigma). The flag eluents were subsequently subjected to western blot analysis using anti-E2F8 antibody (M01, Abnova). All nuclear extraction and immunoaffinity purification steps were performed at 4°C and fresh protease inhibitors were added to all working solutions.

ChIP and Sequential ChIP Assays

For ChIP assays, the EZ CHIP assay kit (Upstate) was used as described by the manufacturer. In brief, harvested HEK293 cells overexpressing flag-E2F7 and/or flag-E2F8 were crosslinked and chromatin was sonicated to an average size of 200–1000 bp. Lysates were subsequently precleared with Salmon Sperm DNA/Protein G agarose slurry. Antibodies specific to flag, HA, or normal mouse IgG (Oncogene) were then added to each sample and incubated overnight at 4°C. Antibody-protein-DNA complexes were recovered by addition of 30 μl of Salmon Sperm DNA/Protein G agarose slurry and incubation for 1 hr at 4°C. Following extensive washing, the complexes were eluted and decrosslinked at 65°C for 4 hr. Finally, samples were treated with Proteinase K (Roche) and Rnase A (Roche) and purified through Qiaquick columns (QIAGEN). Real-time PCR quantification of immunoprecipitated DNA was performed using the Biorad iCycler machine with primers specific for the indicated promoter regions. All primer sequences are listed in Figure S7. Reactions were performed in triplicate and normalized to 1% of the total input.

Sequential ChIP-PCR was carried out similarly using the same EZ CHIP protocol, except two rounds of chromatin immunoprecipitation steps were performed. The first round of immunoprecipitation was performed by incubation of extracts with M2 anti-flag antibody and Salmon Sperm DNA/Protein G agarose slurry. Precipitated DNA-protein complexes were eluted with excess flag peptide (200 μg/ml) for 1 hr at 4°C and then subjected to a second round of precipitation with primary antibodies as indicated in Figures 3H–3J. Sequentially precipitated complexes were recovered by addition of 30 μl of Salmon Sperm DNA/Protein G agarose slurry and incubation for another 1 hr at 4°C. After extensive washing, protein-DNA complexes collected from sequential ChIP were treated and subjected to real-time PCR analysis as described above for ChIP experiments.

Western Blot and Antibodies

Immunoblot analyses were performed by standard procedures using ECL reagents as described by the manufacturer (Amersham Biosciences). The following commercial antibodies were used as indicated in the figures: flag (M2, Sigma), HA (12C5A, Roche), Myc (9E10, Santa Cruz), E2F1 (C-20, Santa Cruz), tubulin (T6199, Sigma), caspase-3 (9662, Cell Signaling), and p53 (Ab-1, Oncogene).

Cell Culture and Viability Assay

E2f7$^{loxp/loxp}$*E2f8*$^{loxp/loxp}$ mouse embryo fibroblasts (MEFs) were isolated from E13.5 embryos and maintained in DMEM medium containing 15% fetal bovine serum (FBS). Immortalized cell lines were generated from primary MEFs using the standard 3T9 protocol. Immortalized MEFs were treated with retrovirus expressing *cre* recombinase using standard methods (Wu et al., 2001).

Apoptosis was measured in MEFs at the indicated times following treatment with 10 μm cisplatin (Sigma) or 20 μm camptothecin (Sigma) for 18 hr. Cell viability was determined by trypan blue exclusion.

Reporter Assay

Luciferase reporter assays were performed in triplicate as described previously (de Bruin et al., 2003). In brief, cre-treated wild-type and *E2f7*$^{loxP/loxP}$ *E2f8*$^{loxP/loxP}$ MEFs were transfected with *E2f1-Luc* reporter plasmid (Araki et al., 2003), along with a thymidine kinase renilla luciferase construct as an internal control. Cells were harvested and luciferase activity was detected using dual luciferase system (Promega) following the manufacturer's protocol.

FACS Analysis

Cre-treated wild-type and *E2f7*$^{loxP/loxP}$*E2f8*$^{loxP/loxP}$ MEFs were synchronized by starvation in DMEM containing 0.2% FBS for 48 hr and blocked at the G_1/S transition by the addition of DMEM containing 15% FBS with 1 mM hydroxyurea (HU) for 18 hr. Cells were then washed three times with PBS and incubated with fresh medium containing 15% FBS. Cells were harvested at the indicated time points and fixed in 70% ethanol, followed by incubation in propidium iodide and analysis by flow cytometry using standard methods.

BrdU and TUNEL Assays

Pregnant females at 9.5 days postcoitum were injected intraperitoneally with BrdU (100 μg/grams of body weight) 30 min prior to harvesting. Embryos were fixed in formalin and 5 μm paraffin embedded-sections were used for immunohistochemistry. After deparaffinization, anti-BrdU antibody (MO-0744, DAKO) and Vectastain Elite ABC reagents (Vector labs) were used to detect BrdU incorporation according to the manufacturer's instructions. Apoptotic cells were detected using TUNEL (S7101, Chemican) assays, performed according to the manufacturer's protocol. All slides were counterstained with hematoxylin.

Supplemental Data

Supplemental Data include seven figures and one table and can be found with this article online at http://www.developmentalcell.com/cgi/content/full/14/1/62/DC1/.

ACKNOWLEDGMENTS

We are grateful for technical assistance provided by J. Moffitt and J. Opavska. We also thank members of the Leone lab for helpful suggestions and Pam Wenzel for critical reading of the manuscript. This work was funded by NIH grants to G.L. (R01CA85619, R01CA82259, R01HD047470, P01CA097189), an NIH grant to M.W. (R01HD42619), and a DoD award to A.d.B. (BC030892). G.L. is the recipient of The Pew Charitable Trust Scholar Award and the Leukemia & Lymphoma Society Scholar Award. The authors declare that they have no competing financial interests.

Received: July 10, 2007
Revised: October 1, 2007
Accepted: October 30, 2007
Published: January 14, 2008

REFERENCES

Araki, K., Nakajima, Y., Eto, K., and Ikeda, M.A. (2003). Distinct recruitment of E2F family members to specific E2F-binding sites mediates activation and repression of the E2F1 promoter. Oncogene *22*, 7632–7641.

Attwooll, C., Lazzerini Denchi, E., and Helin, K. (2004). The E2F family: specific functions and overlapping interests. EMBO J. *23*, 4709–4716.

Bracken, A.P., Ciro, M., Cocito, A., and Helin, K. (2004). E2F target genes: unraveling the biology. Trends Biochem. Sci. *29*, 409–417.

Christensen, J., Cloos, P., Toftegaard, U., Klinkenberg, D., Bracken, A.P., Trinh, E., Heeran, M., Di Stefano, L., and Helin, K. (2005). Characterization of E2F8, a novel E2F-like cell-cycle regulated repressor of E2F-activated transcription. Nucleic Acids Res. *33*, 5458–5470.

de Bruin, A., Maiti, B., Jakoi, L., Timmers, C., Buerki, R., and Leone, G. (2003). Identification and characterization of E2F7, a novel mammalian E2F family member capable of blocking cellular proliferation. J. Biol. Chem. *278*, 42041–42049.

DeGregori, J., and Johnson, D.G. (2006). Distinct and overlapping roles for E2F family members in transcription, proliferation and apoptosis. Curr. Mol. Med. *6*, 739–748.

DeGregori, J., Leone, G., Miron, A., Jakoi, L., and Nevins, J.R. (1997). Distinct roles for E2F proteins in cell growth control and apoptosis. Proc. Natl. Acad. Sci. USA *94*, 7245–7250.

Dignam, J.D., Lebovitz, R.M., and Roeder, R.G. (1983). Accurate transcription initiation by RNA polymerase II in a soluble extract from isolated mammalian nuclei. Nucleic Acids Res. *11*, 1475–1489.

Di Stefano, L., Jensen, M.R., and Helin, K. (2003). E2F7, a novel E2F featuring DP-independent repression of a subset of E2F-regulated genes. EMBO J. *22*, 6289–6298.

Dimova, D.K., and Dyson, N.J. (2005). The E2F transcriptional network: old acquaintances with new faces. Oncogene *24*, 2810–2826.

Dynlacht, B.D., Flores, O., Lees, J.A., and Harlow, E. (1994). Differential regulation of E2F transactivation by cyclin/cdk2 complexes. Genes Dev. *8*, 1772–1786.

Field, S.J., Tsai, F.Y., Kuo, F., Zubiaga, A.M., Kaelin, W.G., Jr., Livingston, D.M., Orkin, S.H., and Greenberg, M.E. (1996). E2F–1 functions in mice to promote apoptosis and suppress proliferation. Cell *85*, 549–561.

Gaubatz, S., Lindeman, G.J., Ishida, S., Jakoi, L., Nevins, J.R., Livingston, D.M., and Rempel, R.E. (2000). E2F4 and E2F5 play an essential role in pocket protein-mediated G1 control. Mol. Cell *6*, 729–735.

Giangrande, P.H., Zhu, W., Schlisio, S., Sun, X., Mori, S., Gaubatz, S., and Nevins, J.R. (2004). A role for E2F6 in distinguishing G1/S- and G2/M-specific transcription. Genes Dev. *18*, 2941–2951.

Hsieh, J.K., Yap, D., O'Connor, D.J., Fogal, V., Fallis, L., Chan, F., Zhong, S., and Lu, X. (2002). Novel function of the cyclin A binding site of E2F in regulating p53-induced apoptosis in response to DNA damage. Mol. Cell. Biol. *22*, 78–93.

Humbert, P.O., Rogers, C., Ganiatsas, S., Landsberg, R.L., Trimarchi, J.M., Dandapani, S., Brugnara, C., Erdman, S., Schrenzel, M., Bronson, R.T., et al. (2000a). E2F4 is essential for normal erythrocyte maturation and neonatal viability. Mol. Cell *6*, 281–291.

Humbert, P.O., Verona, R., Trimarchi, J.M., Rogers, C., Dandapani, S., and Lees, J.A. (2000b). E2f3 is critical for normal cellular proliferation. Genes Dev. *14*, 690–703.

Kosugi, S., and Ohashi, Y. (2002). E2Ls, E2F-like repressors of *Arabidopsis* that bind to E2F sites in a monomeric form. J. Biol. Chem. *277*, 16553–16558.

Lakso, M., Pichel, J.G., Gorman, J.R., Sauer, B., Okamoto, Y., Lee, E., Alt, F.W., and Westphal, H. (1996). Efficient in vivo manipulation of mouse genomic sequences at the zygote stage. Proc. Natl. Acad. Sci. USA *93*, 5860–5865.

Leone, G., DeGregori, J., Yan, Z., Jakoi, L., Ishida, S., Williams, R.S., and Nevins, J.R. (1998). E2F3 activity is regulated during the cell cycle and is required for the induction of S phase. Genes Dev. *12*, 2120–2130.

Lindeman, G.J., Dagnino, L., Gaubatz, S., Xu, Y., Bronson, R.T., Warren, H.B., and Livingston, D.M. (1998). A specific, nonproliferative role for E2F–5 in choroid plexus function revealed by gene targeting. Genes Dev. *12*, 1092–1098.

Logan, N., Delavaine, L., Graham, A., Reilly, C., Wilson, J., Brummelkamp, T.R., Hijmans, E.M., Bernards, R., and La Thangue, N.B. (2004). E2F–7: a distinctive E2F family member with an unusual organization of DNA-binding domains. Oncogene *23*, 5138–5150.

Logan, N., Graham, A., Zhao, X., Fisher, R., Maiti, B., Leone, G., and La Thangue, N.B. (2005). E2F–8: an E2F family member with a similar organization of DNA-binding domains to E2F–7. Oncogene *24*, 5000–5004.

Maiti, B., Li, J., de Bruin, A., Gordon, F., Timmers, C., Opavsky, R., Patil, K., Tuttle, J., Cleghorn, W., and Leone, G. (2005). Cloning and characterization of mouse E2F8, a novel mammalian E2F family member capable of blocking cellular proliferation. J. Biol. Chem. *280*, 18211–18220.

Mariconti, L., Pellegrini, B., Cantoni, R., Stevens, R., Bergounioux, C., Cella, R., and Albani, D. (2002). The E2F family of transcription factors from *Arabidopsis thaliana*. Novel and conserved components of the retinoblastoma/E2F pathway in plants. J. Biol. Chem. *277*, 9911–9919.

Marti, A., Wirbelauer, C., Scheffner, M., and Krek, W. (1999). Interaction between ubiquitin-protein ligase SCFSKP2 and E2F–1 underlies the regulation of E2F–1 degradation. Nat. Cell Biol. *1*, 14–19.

Muller, H., and Helin, K. (2000). The E2F transcription factors: key regulators of cell proliferation. Biochim. Biophys. Acta *1470*, M1–M12.

Murga, M., Fernandez-Capetillo, O., Field, S.J., Moreno, B., Borlado, L.R., Fujiwara, Y., Balomenos, D., Vicario, A., Carrera, A.C., Orkin, S.H., et al. (2001). Mutation of E2F2 in mice causes enhanced T lymphocyte proliferation, leading to the development of autoimmunity. Immunity *15*, 959–970.

O'Donnell, K.A., Wentzel, E.A., Zeller, K.I., Dang, C.V., and Mendell, J.T. (2005). c-Myc-regulated microRNAs modulate E2F1 expression. Nature *435*, 839–843.

Ogawa, H., Ishiguro, K., Gaubatz, S., Livingston, D.M., and Nakatani, Y. (2002). A complex with chromatin modifiers that occupies E2F- and Myc-responsive genes in G0 cells. Science *296*, 1132–1136.

Pomerantz, J., Schreiber-Agus, N., Liegeois, N.J., Silverman, A., Alland, L., Chin, L., Potes, J., Chen, K., Orlow, I., Lee, H.W., et al. (1998). The Ink4a tumor suppressor gene product, p19Arf, interacts with MDM2 and neutralizes MDM2's inhibition of p53. Cell *92*, 713–723.

Reis, T., and Edgar, B.A. (2004). Negative regulation of dE2F1 by cyclin-dependent kinases controls cell cycle timing. Cell *117*, 253–264.

Rempel, R.E., Saenz-Robles, M.T., Storms, R., Morham, S., Ishida, S., Engel, A., Jakoi, L., Melhem, M.F., Pipas, J.M., Smith, C., et al. (2000). Loss of E2F4 activity leads to abnormal development of multiple cellular lineages. Mol. Cell *6*, 293–306.

Resnitzky, D., Gossen, M., Bujard, H., and Reed, S.I. (1994). Acceleration of the G1/S phase transition by expression of cyclins D1 and E with an inducible system. Mol. Cell. Biol. *14*, 1669–1679.

Riddle, R.D., Johnson, R.L., Laufer, E., and Tabin, C. (1993). Sonic hedgehog mediates the polarizing activity of the ZPA. Cell *75*, 1401–1416.

Rogoff, H.A., Pickering, M.T., Debatis, M.E., Jones, S., and Kowalik, T.F. (2002). E2F1 induces phosphorylation of p53 that is coincident with p53 accumulation and apoptosis. Mol. Cell. Biol. *22*, 5308–5318.

Russell, J.L., Powers, J.T., Rounbehler, R.J., Rogers, P.M., Conti, C.J., and Johnson, D.G. (2002). ARF differentially modulates apoptosis induced by E2F1 and Myc. Mol. Cell. Biol. *22*, 1360–1368.

Saavedra, H.I., Wu, L., de Bruin, A., Timmers, C., Rosol, T.J., Weinstein, M., Robinson, M.L., and Leone, G. (2002). Specificity of E2F1, E2F2, and E2F3 in mediating phenotypes induced by loss of Rb. Cell Growth Differ. *13*, 215–225.

Seville, L.L., Shah, N., Westwell, A.D., and Chan, W.C. (2005). Modulation of pRB/E2F functions in the regulation of cell cycle and in cancer. Curr. Cancer Drug Targets *5*, 159–170.

Stevens, C., and La Thangue, N.B. (2004). The emerging role of E2F–1 in the DNA damage response and checkpoint control. DNA Repair (Amst.) *3*, 1071–1079.

Storre, J., Elsasser, H.P., Fuchs, M., Ullmann, D., Livingston, D.M., and Gaubatz, S. (2002). Homeotic transformations of the axial skeleton that accompany a targeted deletion of E2f6. EMBO Rep. *3*, 695–700.

Wu, L., Timmers, C., Maiti, B., Saavedra, H.I., Sang, L., Chong, G.T., Nuckolls, F., Giangrande, P., Wright, F.A., Field, S.J., et al. (2001). The E2F1–3 transcription factors are essential for cellular proliferation. Nature *414*, 457–462.

Yamasaki, L., Jacks, T., Bronson, R., Goillot, E., Harlow, E., and Dyson, N.J. (1996). Tumor induction and tissue atrophy in mice lacking E2F–1. Cell *85*, 537–548.

Ziebold, U., Reza, T., Caron, A., and Lees, J.A. (2001). E2F3 contributes both to the inappropriate proliferation and to the apoptosis arising in Rb mutant embryos. Genes Dev. *15*, 386–391.